

## Reference test object for on site HIRF test set up verification

W. Quenum, J.P. Parmantier, O. Verstraete, D. Lemaire, F. Therond

► **To cite this version:**

W. Quenum, J.P. Parmantier, O. Verstraete, D. Lemaire, F. Therond. Reference test object for on site HIRF test set up verification. EMC Europe 2014, Sep 2014, GOTHEMBURG, Sweden. <hal-01071570>

**HAL Id: hal-01071570**

**<https://hal-onera.archives-ouvertes.fr/hal-01071570>**

Submitted on 6 Oct 2014

**HAL** is a multi-disciplinary open access archive for the deposit and dissemination of scientific research documents, whether they are published or not. The documents may come from teaching and research institutions in France or abroad, or from public or private research centers.

L'archive ouverte pluridisciplinaire **HAL**, est destinée au dépôt et à la diffusion de documents scientifiques de niveau recherche, publiés ou non, émanant des établissements d'enseignement et de recherche français ou étrangers, des laboratoires publics ou privés.

# Reference test object for on site HIRF test set up verification

## Controlling measurement of EM transfer functions on aircraft

Wilfrid.Quenum<sup>1</sup>, Jean Philippe Parmantier<sup>1</sup>, Olivier Verstraete<sup>2</sup>, Dominique Lemaire<sup>2</sup>, Frédéric Therond<sup>2</sup>

<sup>1</sup> ONERA/DEMR, The French Aerospace Lab, Toulouse, France, [wilfrid.quenum@onera.fr](mailto:wilfrid.quenum@onera.fr)

<sup>2</sup> AIRBUS GROUP: AIRBUS Operations S.A.S, Toulouse, France

**Abstract**— In this paper we propose a simple reference test object which is to be used as a set up verification device to be tested before High Intensity Radiated Frequency (HIRF) measurement campaigns on aircraft. This reference object has been designed to take into account both EM and mechanical requirements. It therefore ensures a good level of sensitivity and reproducibility of a reference measured transfer function between the incident E-field and an internal induced current. This object has been calibrated in laboratory using a strip-line which enables to fully control the incident EM field. Finally tests in open test site conditions have been carried out in order to provide reference transfer functions.

**Key words:** HIRF; strip-line; EM field; Verification; Calibration; Induced currents; Transfer functions

### I. INTRODUCTION

Part of HIRF certification test campaigns consist in measuring “transfer functions” on aircraft in order to be able to verify the EM levels specified for equipment qualification. Because they require the availability of the aircraft, such tests have to be performed in a tight schedule and therefore with a perfect control of emission and measurement system. However, getting this full control is not that obvious because the deployment of the emission system and the whole measurement links on open site are potential sources of errors.

In this context, AIRBUS group proposed to design and to “calibrate” a standard object equipped with cables that would be used before HIRF tests on aircraft to check that the whole emission/measurement system is operating correctly and is able to provide transfer-functions within specified bounds. Those bounds are expressed as levels of transfer functions to be obtained between an incident free field,  $E_{inc}$ , and a current on an electric wire. The dynamic range specified by the AIRBUS group ranged from 0.01mA / (V/m) to 1mA / (V/m) between 30MHz and 400MHz.

The process to obtain the required test-object goes through the following steps:

- The test object is designed from mechanical and EM requirements.
- Then it is calibrated in terms of transfer function in well-controlled laboratory conditions.

- Finally it is tested in a real open test site area to assess the robustness of the resulting transfer function compared to laboratory conditions.
- At the end, reference transfer function bounds can be provided taking into account the sensitivity to various installation parameters.
- These data are used as guidelines for the operator to decide whether the emission/measurement system operates properly or not.

### II. DEFINITION AND DESIGN OF THE REFERENCE BOX

#### A. Requirements on Reference Box

The test-object must be reasonably simple, easy to handle and robust to small shocks. In order to ensure a good reproducibility it must allow easy control of EM coupling in terms of field penetration and induced current on its wiring. This is the reason why we defined the object as a simple perfectly conducting parallelepiped box, later on called “reference box” (RB), with a single aperture and equipped with an internal test-wire. Moreover, we specify in advance that the design achieved is such that small mechanical deformations will have no influence on the results. The aperture, which must be the only point of entry of the incident energy into the system, has to be chosen large enough in order to induce sufficient parasitic coupling onto the test-wire. Nevertheless, in order to comply with the analytical approach needed for supporting the design of the RB and for having a good confidence in the results, the aperture is chosen small enough to assume that the EM fields onto the aperture will be quite homogeneous in the frequency bandwidth of interest.

#### B. Pre-definition of the reference box

First definitions of the dimensions of the box, aperture and test-wire were derived from analytical formulas available in the literature, using K. Lee’s model of EM coupling of a wire under a small aperture ([1], [2]). Nevertheless, before manufacturing the RB, its dimensions have been validated by 3D numerical simulations in order to confirm that the structure would fulfil the transfer function dynamic range requirements. The 3D numerical simulations have been carried out with ONERA’s ALICE FDTD computer code by considering that

the perfectly conducting box was illuminated by a plane wave with a grazing incidence and vertical polarization, and placed at 1.5m above a perfectly metallic ground plane (Figure 1). The resulting transfer function between the current at one extremity of the test-wire and the incident electric field is plotted in Figure 1 and attests that the required dynamic range is reached with this structure. This dynamic range includes the amplitude of the variations of resonances and zeros due to the dimensions of the test-wire and the enclosure.

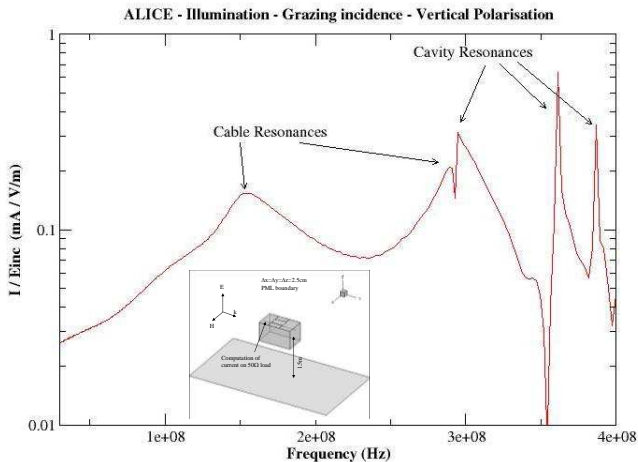


Figure 1: 3D FDTD numerical simulation and calculated  $I/E_{inc}$  transfer function

Consequently it was decided that the RB could be designed with the following characteristics:

- External dimensions: 1m x 0.6m x 0.6m
- Aperture: 0.35m x 0.2m on the top face
- Internal test-wire: 2.5 mm<sup>2</sup> cross-section, 1m long and 10-cm height, running below the aperture, loaded at both ends with a 50 Ohms load.

### C. Structure design

The manufactured RB is assembled with rivets. 0.43m x 0.29m lateral rectangular trapdoors have been designed in order to provide access to the operator inside the box Figure 2.

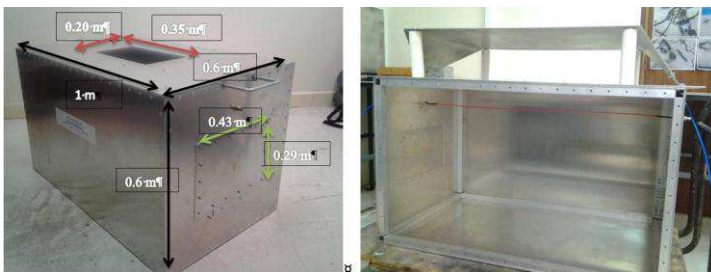


Figure 2: The Reference Box

## III. EXPERIMENTAL STRIP-LINE VALIDATION

### A. Design and calibration of the strip-line

In laboratory conditions, it is essential to have an easy handle and fully controlled illumination system. Such features have been obtained by exciting the RB top aperture with a strip-line installed over the aperture.

The strip-line mounted on the top lid of the box is pictured in Figure 3. The height ( $h_{strip}=0.155m$ ) and dimensions of the strip-line have been chosen in order to preserve as much as possible a 50 Ohms matching in the frequency bandwidth of interest (up to 400MHz) as well as a homogeneous illumination of the aperture.

As a first step, the strip-line has been calibrated in terms of S-parameters between its two extremities. The reflection and transmission parameters,  $S_{11}$ ,  $S_{22}$  and  $S_{21}$ , of the strip-line when the upper trap-door is closed or open are drawn in Figure 4. These plots show that the strip-line has been correctly designed. Indeed  $S_{11}$  is similar to  $S_{22}$  which proves symmetry and  $S_{21}$  shows a smooth variation versus frequency, which proves no significant mismatching in the frequency range of interest.

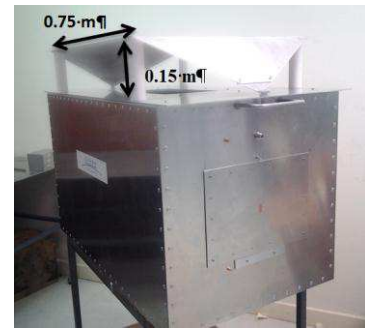


Figure 3: Scheme of the strip-line onto the RB

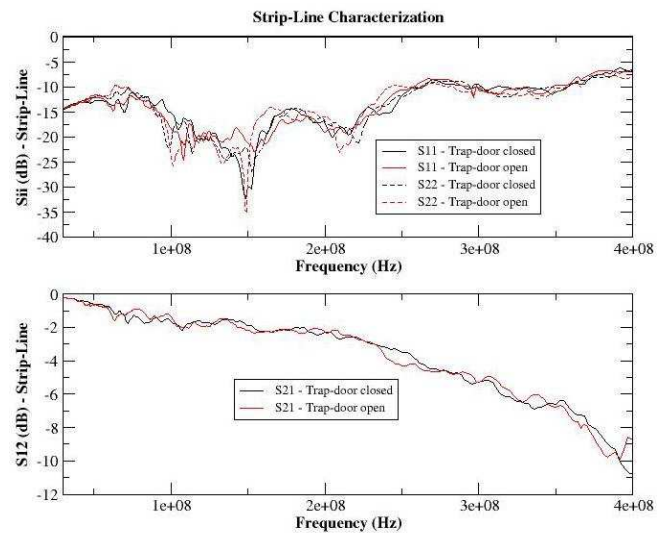


Figure 4: Reflection  $S_{11}$ ,  $S_{22}$  and Transmission  $S_{21}$  parameters of the RB strip-line

## B. Electromagnetic response of RB with the strip-line illumination

### a) Current measurement with the current probe

The next step consists in measuring the induced current at the extremity of the test-wire when the structure is excited by the strip-line. In order to guarantee reproducibility of the measurement of the transfer function, we defined two requirements of the setup. First we identified that it was necessary to ground the probe on a dedicated metallic bracket at the level of the probe connector therefore minimizing any induced parasitic signal. Second, we fixed the length of the measurement cable to 50 cm in order to impose its routing up to the wall SMA transitions towards the measurement apparatus (Figure 5), therefore minimizing EM coupling between the measurement cable and the test-wire. These set-up requirements have to be applied for tests on real test sites (see in Figure 7 the inconsistent transfer function response obtained when the probe is not installed onto the bracket).

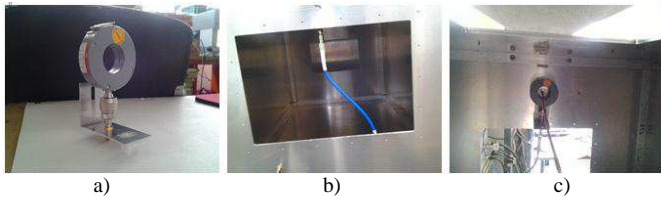


Figure 5: Installation of the current probe: a) the current probe on its metallic bracket, b) the measurement cable seen from the side trap-door (in blue), c) the measurement cable and the current probe seen from inside the RB

### b) Reference laboratory measurement of the transfer function

In the reference configuration, the upper trap-door of the aperture is opened (Figure 6). The transfer function between the current onto the test-wire and the short-circuit electric field onto the aperture,  $E_{sc}$  (the electric field when the trap-door is closed) results to be a very stable quantity that can be deduced from the measurement of the S-parameters between the input of the strip-line and the output of the current probe.

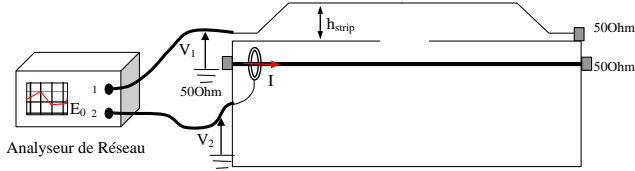


Figure 6: Set-up for the measurement of S-parameters between the RB strip-line input and the current probe output

Since we can assume the strip-line works properly between 30MHz and 400MHz; the E-field generated onto the aperture is deduced from “(1)” considering the absence of resonance and taking into account the mismatching of the strip-line. At the end, the transfer function can be expressed as a function of the measurement of  $S_{21}$  between the probe and the strip-line and the  $S_{11}$  of the strip-line as reported in “(2)” in which  $Z_t$  is the transfer impedance of the current probe:

$$E_{sc}^{IV,theo} = \frac{(1 + S_{11})}{2h_{strip}} \quad (1)$$

$$\frac{I}{E_{sc}} = \frac{S_{21}^{probe} \cdot h_{strip}}{Z_t \cdot (1 + S_{11})} \quad (2)$$

Even if in this configuration we consider the short-circuited electric field on the aperture,  $E_{sc}$ , this transfer function measured in the strip-line (Figure 7) is fully consistent with the result observed in 3D simulation in terms of frequency shape (order of magnitude and test-wire and enclosure frequency resonances) especially for frequencies over 360 MHz (Figure 1). Note that we verified that  $E_{sc}$  can also be taken close to the aperture when this one is opened.

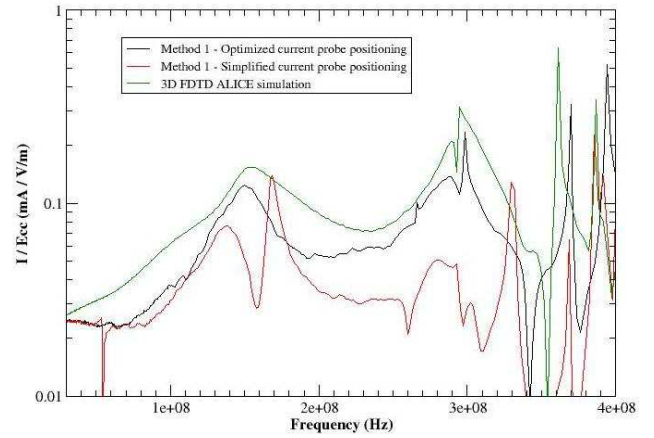


Figure 7:  $I/E_{sc}$  transfer function between the induced current and the surface E-field onto the aperture in the strip-line – comparison with “reference” simulation result - advantage of using the bracket device to support the current probe

## IV. ILLUMINATION OF THE RB IN AN OPEN AIR TEST SITE

The next step consists in measuring the transfer function between the current induced onto the internal test-wire and the incident free electric field in open air test site (OATS) conditions. In this test, the instrumentation is the one usually used by the Airbus Group in HIRF measurement campaigns. An antenna is driven by an amplifier and a synthesiser which provide the required incident field in the [30MHz – 400MHz] frequency range according to AIRBUS’s practises for such tests... Current measurements are performed with current probes, optical fiber links and a spectrum analyser.

In order to minimize as much as possible the effect of the ground for our transfer function measurement, it has been decided to consider a horizontal polarization of the antenna. Nevertheless the adequacy of the required dynamic range of the transfer function remains conditioned by the fact that we still apply the same local conditions of incident electric field on the aperture. Consequently, the RB must also be turned 90 degrees in the test area (the aperture is now on the side of the RB) as illustrated in Figure 8 in order to maintain the same configuration of EM coupling as in the strip-line test or as in the 3D simulation.

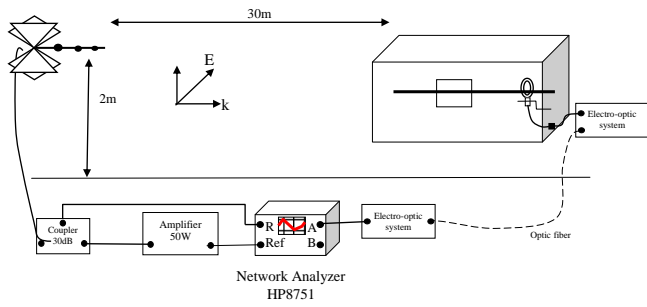


Figure 8: Experimental procedure on OATS

Various tests have been carried out in order to qualify and quantify the level of sensitivity of the measured transfer function taking into account various parameters: the reproducibility of measurements performed by different operators, the influence of the type of current probes and the influence of the incidence illumination angle onto the RB. Figure 9 displays a typical transfer function measured in Airbus's OATS in Toulouse ( $I/E_{inc}$ ) and a comparison to the strip-line configuration ( $I/E_{sc}$ ).

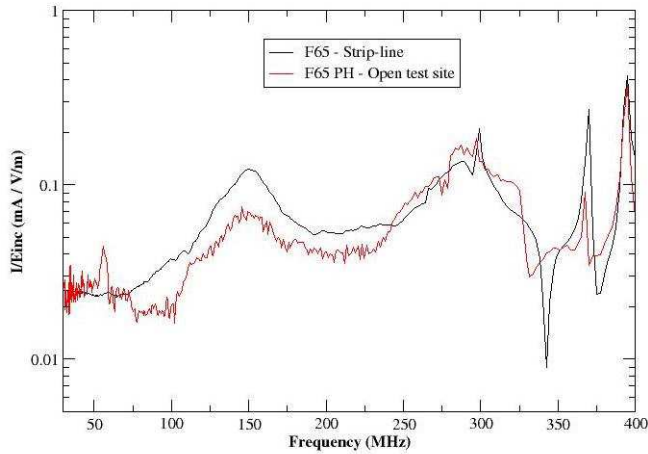


Figure 9:  $I/E_{inc}$  transfer function in OATS and in strip-line

## V. DEFINITION OF REFERENCE TRANSFER FUNCTION BOUNDS

As seen for all available results, the transfer functions of induced current on the RB test-wire versus the incident electric field or versus the short-circuited electric field show very specific signatures:

- A low frequency variation from 30MHz up to 250MHz with a high level of reproducibility;
- Two test-wire resonances around 150MHz ( $f_{TL1}$ ) and around 300MHz ( $f_{TL2}$ ) with low quality factors;
- A domain of resonances above 300MHz with three characteristic enclosure resonances ( $f_{B1}$ ,  $f_{B2}$ ,  $f_{B3}$ ) with high quality factors. The first resonance frequency with high quality factor,  $f_{B1}$ , overlays the second transmission line resonance of the test-wire with low quality factor,  $f_{TL2}$ .

- A set of 2 possible zeros with a low level of reproducibility depending on the type of current probe used for the current measurement. These frequencies have a large range of possible values.

Consequently, the variability of reference  $I/E_{inc}$  transfer functions characterizing EM coupling onto the RB is summarized by a set of three curves as plotted in Figure 10. The three curves (average transfer function, upper bound and lower bound) take into account typical degree of reproducibility and possible deviation due to the type of current probes or angles incidence of the illumination on the RB.

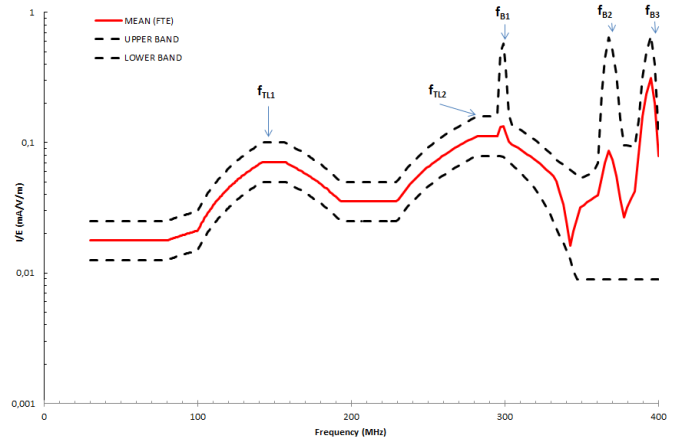


Figure 10: Reference data of  $I/E_{inc}$  transfer functions (Average, Lower and Upper bounds) for an illumination of the RB in nominal configuration

In Figure 11, Figure 12 and Figure 13, we show examples of results leading to acceptance or rejection of the validation of the emission/measurement system. In Figure 11, the measurement is validated because it remains globally within the bounds of the transfer functions even if at some specific frequencies (about 50MHz, 85MHz) peaks may exceed the upper boundary and if some zeros are observed at 360 MHz. In Figure 12, the measurement is out of the bounds of the transfer functions in the resonance region. Especially the  $f_{B1}$ ,  $f_{B2}$  and  $f_{B3}$  resonance frequencies are not well marked and zeros appear outside the resonance region (250MHz). Such a signature as in Figure 12 is typical of a problem of installation of the current probe in the RB (connector not sufficiently grounded). In Figure 13, a functional failure has been introduced on purpose to test the measurement link. Even if the goal of the RB is not primarily to detect functional upsets of measurement equipment since each one is verified separately before a test campaign, the RB can provide a complementary check prior to the test; in Figure 13 the measurement is clearly out of the bounds of the transfer functions below the resonance region ( $f < 250$  MHz) and commands to check the measurement link.

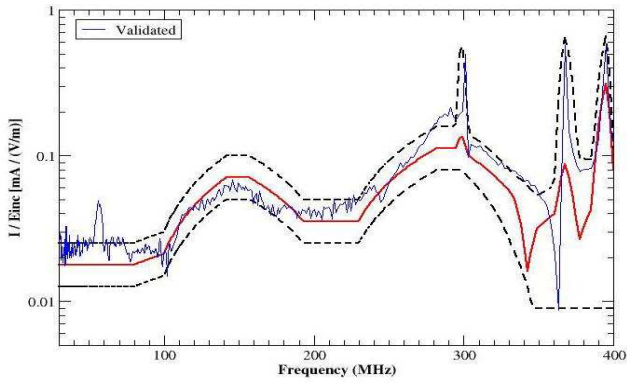


Figure 11: Validated measurement

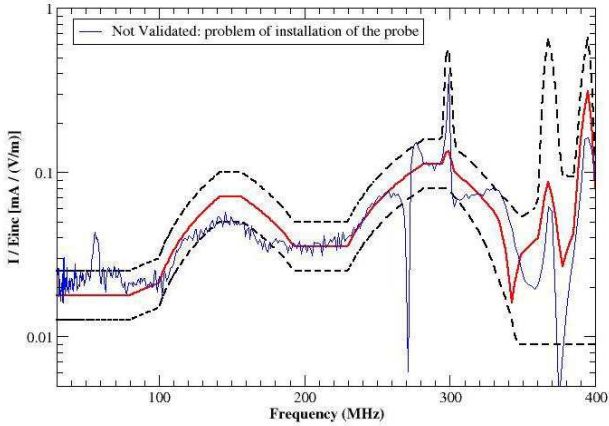


Figure 12: Rejected measurement because of bad grounding of the current probe

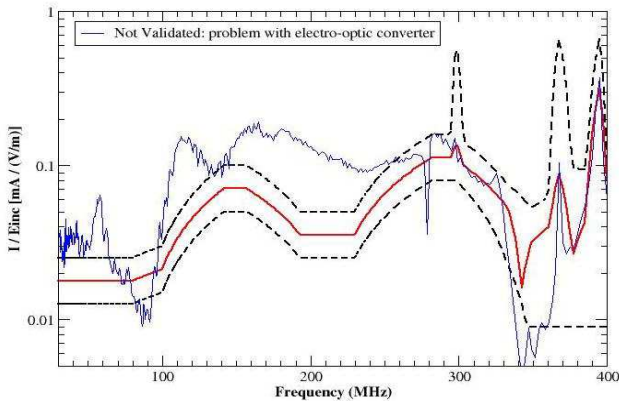


Figure 13: Rejected measurement because of fault on the measurement link

## CONCLUSION

The RB has been defined, designed and built in order to verify the capability to measure HIRF  $I/E_{inc}$  transfer functions (induced current over incident electric field in a configuration of illumination) with the required dynamic range between 30MHz and 400MHz frequency band. This device is meant to serve as a “sanity check” of the test equipment prior to any aircraft level test campaigns. The RB measurement set-up is thereby fully controlled in order to obtain the best level of reproducibility, and provides some diagnosis means of potential errors. In addition, a strip-line allows a pre-calibration of such EM coupling in a controlled laboratory environment which may be used as a non-regression test in order to check the integrity of the reference box in case of doubt on the RB results.

The way to operate the RB in laboratory in order to obtain reference  $I/E$  transfer functions is comparable to usual practices with current/current measurement jigs. Nevertheless, so far, the RB is planned to be used for HIRF verification tests only. Indeed, the results presented in this paper concern a specific OATS and they need to be confirmed by a larger exploitation on different OATSs.

## REFERENCE

- [1] K.S.H. LEE : EMP Interaction: principles, techniques and reference data, Hemisphere Publishing Corporation, Washington, New York, London, 1986.
- [2] J-P. Parmantier, P. Degauque : “Topology Based Modeling of Very Large Systems”. Modern radio Science 1996. Edited by J. Hamelin. Oxford University Press. pp. 151-177
- [3] J-P. Parmantier : “S-parameter determination with a pair of current injection and measurement probes”. Interaction Notes. Note 552. October 1998\*
- [4] J-P. Parmantier, V. Gobin Chapitre 3 : « Pénétration et couplage dans les structures tridimensionnelles (in French) ». In “EM Compatibility”, Collection technique et scientifique des télécommunications. Lavoisier, Hermes.Paris 2007. under the direction of P. Degauque and A. Zeddani.

\* Interaction notes are available at: <http://www.ece.unm.edu/summa/notes/>